

High order volume-preserving algorithms for relativistic charged particles in general electromagnetic fields

Yang He,^{1,2} Yajuan Sun,³ Ruili Zhang,^{1,2} Yulei Wang,^{1,2} Jian Liu,^{1,2} and Hong Qin^{1,4}

¹*Department of Modern Physics and Collaborative Innovation*

Center for Advanced Fusion Energy and Plasma Sciences,

University of Science and Technology of China, Hefei, Anhui 230026, CHINA

²*Key Laboratory of Geospace Environment,*

CAS, Hefei, Anhui 230026, CHINA

³*LSEC, Academy of Mathematics and Systems Science,*

Chinese Academy of Sciences, P. O. Box 2719, Beijing 100190, CHINA

⁴*Plasma Physics Laboratory, Princeton University,*

Princeton, New Jersey 08543, USA

Abstract

We construct high order symmetric volume-preserving methods for the relativistic dynamics of a charged particle by the splitting technique with processing. Via expanding the phase space to include time t , we give a more general construction of volume-preserving methods that can be applied to systems with time-dependent electromagnetic fields. The newly derived methods provide numerical solutions with good accuracy and conservative properties over long time of simulation. Furthermore, because of the use of processing technique the high order methods are explicit, and cost less than the methods derived from standard compositions, thus are more efficient. The results are verified by the numerical experiments. Linear stability analysis of the methods show that the high order processed method allows larger time step size during integration.

I. INTRODUCTION

The dynamics of relativistic particles under the influence of electromagnetic fields is a fundamental process in plasma physics, space physics, accelerator physics, etc.. Numerical simulations on trajectories of charged particles have been widely used to study their dynamical behaviours. In most multi-scale problems, such as the runaway electron dynamics in tokamaks, and the formation of energetic electrons in magnetosphere, long-term numerical integrations are required to reproduce the entire physical processes. For example, in tokamaks the typical timescale of runaway acceleration process is about 1s, which is 10^8 times larger than its transit period. It is thus essential for the numerical algorithms to give a correct, accurate, and fast long-term simulation in tracking the secular particle trajectory. Conventional methods, such as the fourth order Runge-Kutta method, cannot trace the trajectory accurately after a long time of computation due to the error accumulation. Great advances have been achieved in long-term accurate simulations of charged particle dynamics and Vlasov-Maxwell systems with the application of geometric integration methods [1–17]. Via preserving intrinsic structures of a dynamical system, geometric integration methods [18–21] usually generate numerical results with better accuracy and conservative properties [21, 22].

The relativistic dynamics of a charged particle in the electromagnetic fields \mathbf{E} and \mathbf{B} are governed by

$$\begin{aligned}\frac{d\mathbf{x}}{dt} &= \frac{1}{m_0\gamma(p)}\mathbf{p}, \\ \frac{d\mathbf{p}}{dt} &= q\mathbf{E}(\mathbf{x}, t) + \frac{q}{m_0\gamma(p)}\mathbf{p} \times \mathbf{B}(\mathbf{x}, t),\end{aligned}\tag{1}$$

where \mathbf{x} and \mathbf{p} are the position and momentum vectors, m_0 and q denote the rest mass and charge of the particle, and $\gamma(p) = \sqrt{1 + p^2/(m_0^2c^2)}$ is the Lorentz factor with c the speed of light in vacuum. In Eq. (1), letting $p/c \rightarrow 0$ leads to a non-relativistic Lorentz force equation. Although the physical nature of the relativistic system is different from the non-relativistic system, they have similar geometric properties, that is, the system (1) has the symplectic and volume-preserving properties [7, 17]. It is believed that symplectic methods in general are implicit, and that popular explicit algorithms such as the Boris method is not symplectic [23]. Based on the volume-preserving property, Symmetric Volume-Preserving (SVP) algorithms have been proposed for solving the secular relativistic [9] and non-relativistic [6–8] dynamics

of a charged particle. One of the major properties of these methods is that the volume form in phase space (\mathbf{x}, \mathbf{p}) is invariable along the updating map of the numerical solution $\phi_h : (\mathbf{x}_k, \mathbf{p}_k) \mapsto (\mathbf{x}_{k+1}, \mathbf{p}_{k+1})$, which means the Jacobian

$$\det \left(\frac{\partial(\mathbf{x}_{k+1}, \mathbf{p}_{k+1})}{\partial(\mathbf{x}_k, \mathbf{p}_k)} \right) \equiv 1.$$

Another property is that the methods are time-symmetric, i.e. $\phi_h = \phi_{-h}^{-1}$. The SVP methods have been verified to guarantee the long-term accuracy of numerical solutions and the conservation of the constants of motion such as energy and angular momentum. Moreover, they can be iterated explicitly and implemented easily, thus are efficient in solving the secular trajectories of charged particles, and can be developed as particle solvers in the Particle In Cell (PIC) code [24].

In the current paper, we construct explicit, high order symmetric volume-preserving algorithms for the relativistic dynamics under the general electromagnetic fields. Explicit volume-preserving algorithms can be constructed by the splitting technique [6, 25]. The equations are decomposed as a summation of three incompressible subsystems, and SVP methods are constructed by symmetric compositions of the volume-preserving update mappings that solve the corresponding subsystems. However, when the electromagnetic fields are time-dependent, it is not always trivial to solve the subsystems exactly. Therefore, we append the time t to the dependent variables, it follows that the nonautonomous systems are turned into autonomous ones. In this case, SVP methods can be given for general time-dependent electromagnetic fields by applying the splitting technique to the new system.

As the SVP methods are developed using the splitting technique, it is known that the higher the order of accuracy is, the larger number of mappings is required in the compositions. This generates larger computing amount. To reduce the computation amount over the simulation interval, we employ the processing technique [26, 27] in the construction of high order methods. That is, we derive method in the form $\Psi_h = \chi_h \circ \Phi_h \circ \chi_h^{-1}$, where the kernel Φ_h is the updating mapping given by the usual splitting method, the processor χ_h is a near identity map, and \circ denotes the composition. After N steps of iteration, we have $\Psi_h^N = \chi_h \circ \Phi_h^N \circ \chi_h^{-1}$. From the relation it is easy to see that the computing efforts of Ψ_h mainly comes from Φ_h . A most efficient method can be derived by choosing the kernel method Φ_h as simple as possible, and searching for the processor χ_h to achieve the desired order of accuracy. This idea has been applied to non-relativistic dynamical systems [8]. For

the relativistic dynamics, we split the motion equations in three parts or more, and present a high order SVP method by applying processing. We will show in the numerical experiments and the linear stability analysis that the newly derived high order methods are more efficient than the conventional composition methods, and allow larger step size to satisfy the stability conditions.

This paper is organized as follows. In section 2, we give the derivation of the SVP methods under the general time-dependent electromagnetic fields using the splitting technique with processing. In section 3, we present the study of the linear stability of the SVP methods. In section 4, the newly developed SVP methods are tested by two physical problems, i.e. the penning trap and the problem possessing a plane polarized electromagnetic wave.

II. HIGH ORDER VOLUME-PRESERVING ALGORITHMS

In this section, we give a general derivation of high order volume-preserving algorithms for simulating the relativistic orbits under a time-dependent electromagnetic field by using the splitting and processing technique.

We consider the most general case in which the electromagnetic fields are time-dependent. To apply the splitting and processing technique, we introduce $\sigma = t$ as a new dependent variable, then it follows from (1) that

$$\frac{d}{dt} \begin{pmatrix} \mathbf{x} \\ \mathbf{p} \\ \sigma \end{pmatrix} = \begin{pmatrix} \frac{1}{m_0\gamma(p)}\mathbf{p} \\ q\mathbf{E}(\mathbf{x}, \sigma) + \frac{q}{m_0\gamma(p)}\mathbf{p} \times \mathbf{B}(\mathbf{x}, \sigma) \\ 1 \end{pmatrix}. \quad (2)$$

From Eq. (2), it is known that with the coordinate $(\mathbf{x}, \mathbf{p}, \sigma)$ the system (1) becomes an autonomous system defined in an expanded space $\mathbb{R}^3 \times \mathbb{R}^3 \times \mathbb{R}$ (see Ref. 28 for more details). It is easy to check that the system (2) is source-free, i.e. the divergence of the vector field on the right hand side satisfies

$$\nabla_x \cdot \frac{1}{m_0\gamma(p)}\mathbf{p} + \nabla_p \cdot \left(q\mathbf{E}(\mathbf{x}, \sigma) + \frac{q}{m_0\gamma(p)}\mathbf{p} \times \mathbf{B}(\mathbf{x}, \sigma) \right) + \nabla_\sigma 1 = 0,$$

thus the volume in the expanded phase space is invariant along the exact solution flow. Notice that for any map $\Psi : (\mathbf{x}_k, \mathbf{p}_k, \sigma_k) \mapsto (\mathbf{x}_{k+1}, \mathbf{p}_{k+1}, \sigma_{k+1})$ that preserves volume in the expanded space, the Jacobian satisfies

$$1 = \det \left(\frac{\partial(\mathbf{x}_{k+1}, \mathbf{p}_{k+1}, \sigma_{k+1})}{\partial(\mathbf{x}_k, \mathbf{p}_k, \sigma_k)} \right) = \det \left(\frac{\partial(\mathbf{x}_{k+1}, \mathbf{p}_{k+1})}{\partial(\mathbf{x}_k, \mathbf{p}_k)} \right),$$

if $\frac{\partial \sigma_{k+1}}{\partial \mathbf{x}_k} = \frac{\partial \sigma_{k+1}}{\partial \mathbf{p}_k} = \mathbf{0}$, $\frac{\partial \sigma_{k+1}}{\partial \sigma_k} = 1$. This implies that if the appended variable σ solves $\dot{\sigma} = \text{const}$, volume-preserving methods for source-free systems in the expanded space also preserve the volume of phase space (\mathbf{x}, \mathbf{p}) . This gives us a hint on how to split the system.

Firstly, we split the system (2). It is observed that the system (2) can be decomposed as three source-free solvable subsystems,

$$\begin{aligned} \frac{d}{dt} \begin{pmatrix} \mathbf{x} \\ \mathbf{p} \\ \sigma \end{pmatrix} &= \begin{pmatrix} \frac{1}{m_0 \gamma(p)} \mathbf{p} \\ \mathbf{0} \\ 1 \end{pmatrix} + \begin{pmatrix} \mathbf{0} \\ q \mathbf{E}(\mathbf{x}, \sigma) \\ 0 \end{pmatrix} + \begin{pmatrix} \mathbf{0} \\ \frac{q}{m_0 \gamma(p)} \mathbf{p} \times \mathbf{B}(\mathbf{x}, \sigma) \\ 0 \end{pmatrix} \\ &= F_1(\mathbf{x}, \mathbf{p}, t) + F_2(\mathbf{x}, \mathbf{p}, t) + F_3(\mathbf{x}, \mathbf{p}, t). \end{aligned} \quad (3)$$

The first two subsystems with F_1 and F_2 can be solved exactly by a translation transformation as

$$\phi_h^{F_1} : \begin{cases} \mathbf{x}(t+h) = \mathbf{x}(t) + h \frac{\mathbf{p}(t)}{m_0 \gamma(p(t))}, \\ \mathbf{p}(t+h) = \mathbf{p}(t), \\ \sigma(t+h) = \sigma(t) + h, \end{cases} \quad \phi_h^{F_2} : \begin{cases} \mathbf{x}(t+h) = \mathbf{x}(t), \\ \mathbf{p}(t+h) = \mathbf{p}(t) + h q \mathbf{E}(\mathbf{x}(t), \sigma(t)), \\ \sigma(t+h) = \sigma(t). \end{cases}$$

Here the mappings $\phi_h^{F_i}$, $i = 1, 2, 3$ denote one h -time step updating of the variables. When the third subsystem is concerned, it is noticed that $p^2 = \mathbf{p}^\top \mathbf{p}$ is invariant along the exact solution flow, so as to $\gamma(p)$. Thus, the updating map $\phi_h^{F_3}$ of the exact solution can be calculated as

$$\begin{aligned} \phi_h^{F_3} : \begin{cases} \mathbf{x}(t+h) = \mathbf{x}(t), \\ \mathbf{p}(t+h) = \exp \left(h \frac{q}{m_0 \gamma(p(t))} \hat{\mathbf{B}}(\mathbf{x}(t), \sigma(t)) \right) \mathbf{p}(t), \\ \sigma(t+h) = \sigma(t). \end{cases} \end{aligned} \quad \begin{aligned} &(4a) \\ &(4b) \\ &(4c) \end{aligned}$$

with $\hat{\mathbf{B}} = \begin{bmatrix} 0 & B_3 & -B_2 \\ -B_3 & 0 & B_1 \\ B_2 & -B_1 & 0 \end{bmatrix}$ defined by $\mathbf{B}(\mathbf{x}) = [B_1(\mathbf{x}), B_2(\mathbf{x}), B_3(\mathbf{x})]^\top$. The operator \exp in (4b) is the exponential operator of a matrix, which can be expressed in a closed form for three dimensional skew symmetric matrix as

$$\begin{aligned} \mathbf{p}(t+h) &= \exp \left(h a \hat{\mathbf{B}} \right) \mathbf{p}(t) \\ &= \mathbf{p}(t) + \frac{\sin(haB)}{B} \mathbf{p}(t) \times \mathbf{B} + \frac{(1 - \cos(haB))}{B^2} \mathbf{p}(t) \times \mathbf{B} \times \mathbf{B}. \end{aligned} \quad (5)$$

Here $a = \frac{q}{m_0 \gamma(p(t))}$.

It is easy to prove that each of the mappings $\varphi_h^{F_1}$, $\varphi_h^{F_2}$, $\varphi_h^{F_3}$ preserves the volume in phase space (\mathbf{x}, \mathbf{p}) . Due to the group property, their various compositions provide the SVP methods of any order [21, 29, 30]. As follows, we present some SVP methods of second and fourth orders.

Second order symmetric methods. A second order symmetric method can be derived by the symmetric composition $G_h^2 := \phi_{\frac{h}{2}}^{F_1} \circ \phi_{\frac{h}{2}}^{F_2} \circ \phi_h^{F_3} \circ \phi_{\frac{h}{2}}^{F_2} \circ \phi_{\frac{h}{2}}^{F_1}$

$$\begin{aligned}\mathbf{x}_{k+\frac{1}{2}} &= \mathbf{x}_k + \frac{h}{2} \frac{\mathbf{p}_k}{m_0 \gamma(p_k)}, \\ \mathbf{p}^- &= \mathbf{p}_k + \frac{hq}{2} \mathbf{E}_{k+\frac{1}{2}}, \\ \mathbf{p}^+ &= \exp\left(\frac{hq}{m_0 \gamma(p^-)} \hat{\mathbf{B}}_{k+\frac{1}{2}}\right) \mathbf{p}^-, \\ \mathbf{p}_{k+1} &= \mathbf{p}^+ + \frac{hq}{2} \mathbf{E}_{k+\frac{1}{2}}, \\ \mathbf{x}_{k+1} &= \mathbf{x}_{k+\frac{1}{2}} + \frac{h}{2} \frac{\mathbf{p}_{k+1}}{m_0 \gamma(p_{k+1})},\end{aligned}\tag{6}$$

where $\mathbf{E}_{k+\frac{1}{2}} := \mathbf{E}(\mathbf{x}_{k+\frac{1}{2}}, t_{k+\frac{1}{2}})$, $\mathbf{B}_{k+\frac{1}{2}} := \mathbf{B}(\mathbf{x}_{k+\frac{1}{2}}, t_{k+\frac{1}{2}})$ are the field values evaluated at the position $\mathbf{x}_{k+\frac{1}{2}}$ and the time $t_{k+\frac{1}{2}}$.

If we replace $\phi_h^{F_3}$ with a numerical solution Φ_h of the third subsystem, for example computed by the midpoint method, in symmetric composition G_h^2 , this provides an alternative SVP method of second order

$$\tilde{G}_h^2 := \phi_{\frac{h}{2}}^{F_1} \circ \phi_{\frac{h}{2}}^{F_2} \circ \Phi_h^{F_3} \circ \phi_{\frac{h}{2}}^{F_2} \circ \phi_{\frac{h}{2}}^{F_1}.\tag{7}$$

It recovers the numerical algorithm proposed in Ref. 9.

In a similar way, the higher order SVP methods can be derived via various compositions of approximate (exact) solutions of each subsystems. For example, the fourth order method can be derived by using the well known Yoshida's composition [31] as

$$G_h^4 Y = G_{a_1 h}^2 \circ G_{a_2 h}^2 \circ G_{a_1 h}^2,\tag{8}$$

or by using the Suzuki's fourth order composition as [32]

$$G_h^4 S = G_{b_1 h}^2 \circ G_{b_2 h}^2 \circ G_{b_3 h}^2 \circ G_{b_2 h}^2 \circ G_{b_1 h}^2,\tag{9}$$

where $a_1 = (2 - 2^{1/3})^{-1}$, $a_2 = 1 - 2a_1$, $b_1 = b_2 = (4 - 4^{1/3})^{-1}$, $b_3 = 1 - 2(b_1 + b_2)$. The method $G_h^4 S$ has smaller error constant than the method $G_h^4 Y$. It is clear from (8) and (9)

that the higher order methods produce the numerical solutions of high accuracy, as well as the large computation cost. To reduce the computation cost, we then present the efficient fourth order symmetric SVP methods by employing the processing technique.

The main idea of processing technique is to apply a transformation χ_h called the processor to a known lower order integrator Φ_h such that the new derived method $\tilde{\Phi}_h = \chi_h \circ \Phi_h \circ \chi_h^{-1}$ has a higher order of accuracy than Φ_h . Clearly, $\tilde{\Phi}_h$ maintains all properties (e.g. the long-term stability, structure-preserving property) inherited by the lower order method Ψ_h . After N steps of iteration it is $\tilde{\Psi}_h^N = \chi_h \circ \Psi_h^N \circ \chi_h^{-1}$ which states that using $\tilde{\Psi}_h^N$ does not need more computation cost than Ψ_h . In Ref. 8, processed methods are given when the system is separated into two parts. For the relativistic dynamical system (1) with the splitting (3), the kernel is given by the compositions of $G_h = \phi_h^1 \circ \phi_h^2 \circ \phi_h^3$ and $G_h^* = \phi_h^3 \circ \phi_h^2 \circ \phi_h^1$ as

$$\begin{aligned}\Psi_h &= G_{a_1 h} \circ G_{b_1 h}^* \circ G_{a_2 h} \circ G_{b_2 h}^* \circ \dots \circ G_{a_s h} \circ G_{b_s h}^*, \\ \chi_h &= G_{x_1 h} \circ G_{y_1 h}^* \circ G_{x_2 h} \circ G_{y_2 h}^* \circ \dots \circ G_{x_m h} \circ G_{y_m h}^*,\end{aligned}\tag{10}$$

where $\{a_i, b_i\}_{i=1}^s$ and $\{x_i, y_i\}_{i=1}^m$ are the composition coefficients determined by the order conditions. As an example, we list a fourth order processed method presented in Ref.27.

Fourth order symmetric methods. One of processed composition methods reads

$$G_h^4 P = \chi_h \circ \Psi_h \circ \chi_h^{-1},\tag{11}$$

where Ψ_h and χ_h are in the form (10) with $s = m = 4$, and the composition coefficients are listed in Table I. It is easy to verify that the fourth order method $G_h^4 P$ is symmetric, as $G_h^4 P \circ G_{-h}^4 P(\mathbf{z}) \equiv \mathbf{z}$ holds for any \mathbf{z} .

$a_1 = \frac{\sqrt{18069}-15}{300}$	$b_1 = \frac{6}{25}$
$a_2 = \frac{9}{25}$	$b_2 = -\frac{\sqrt{18069}+15}{300}$
$a_3 = b_2, a_4 = b_1$	$b_3 = a_2, b_4 = a_1$
$x_1 = 0$	$y_1 = 0.1171835753202670$
$x_2 = 0.4731269439352653$	$y_2 = -0.1351671439946886$
$x_3 = 1.350298160490375$	$y_3 = -0.4530449481299280$
$x_4 = 0.05719279780976250$	$y_4 = -0.1930850894788554$

TABLE I. Composition coefficients of the processed method $G_h^4 P$.

III. LINEAR STABILITY ANALYSIS

The linear stability of the SVP methods applied to the non-relativistic dynamics has been analyzed in Ref. 8. In this section, we generalize this study to relativistic dynamics. In order to do this, we first present the test model equation.

Consider the relativistic dynamics of a charged particle in an uniform background magnetic field $\mathbf{B} = B_0\omega\mathbf{e}_z$, and electric field produced by an ideal quadrupole potential distribution,

$$\phi(\mathbf{x}) = \frac{1}{2} \frac{qB_0^2}{m_0} \epsilon (\lambda_x^2 x^2 + \lambda_y^2 y^2 - (\lambda_x^2 + \lambda_y^2) z^2), \quad \lambda_x, \lambda_y > 0, \epsilon = \pm 1.$$

Linearizing system (1) with the above electromagnetic field around $(\mathbf{x}_0, \mathbf{p}_0) \in \mathbb{R}^6$, we get the following equations

$$\dot{\mathbf{x}} = \frac{1}{\gamma_0} \mathbf{p}, \quad \dot{\mathbf{p}} = -\frac{1}{B_0 c} \nabla \phi(\mathbf{x}) + \frac{\mathbf{p}}{\gamma_0} \times \frac{\mathbf{B}}{B_0}, \quad (12)$$

where the variables are dimensionless normalized by $l_0 = m_0 c / (e B_0)$ in space and $(\omega_{ce})^{-1} = m_0 / (q B_0)$ in time, and $\gamma_0 = (\sqrt{1 + p_0^2})^3 > 1$ is a constant. In the linearized system (12), the transverse motion and the axial dynamics are decoupled. As the SVP methods developed in this paper simulate this axial motion exactly, we only need to concentrate on its transverse motion. Set $\lambda^2 = \lambda_x^2 = \lambda_y^2$, and denote $\mathbf{x} = [x, y]$, $\mathbf{p} = [p_x, p_y]$, the two-degree test system is

$$\dot{\mathbf{x}} = \frac{1}{\gamma_0} \mathbf{p}, \quad \dot{\mathbf{p}} = -\epsilon \lambda^2 \mathbf{x} + \frac{\omega}{\gamma_0} J \mathbf{p}, \quad (13)$$

where $J = \begin{pmatrix} 0 & 1 \\ -1 & 0 \end{pmatrix}$ is the standard symplectic matrix.

Applying the SVP methods with time step h to the test system (13), we derive

$$\begin{pmatrix} \gamma_0 \mathbf{x}^{k+1} \\ h \mathbf{p}^{k+1} \end{pmatrix} = M \left(\epsilon \left(\frac{h\lambda}{\sqrt{\gamma_0}} \right)^2, \frac{h\omega}{\gamma_0} \right) \begin{pmatrix} \gamma_0 \mathbf{x}^k \\ h \mathbf{p}^k \end{pmatrix}, \quad (14)$$

where M is the corresponding update matrix depending on $\epsilon(h\lambda/\sqrt{\gamma_0})^2$ and $h\omega/\gamma_0$. For the SVP methods constructed based on the splitting method in Eq.(3), the update matrix M is the production of update matrices for each subsystem. For the second order method $G_h = \phi_{h/2}^{F_1} \circ \phi_{h/2}^{F_2} \circ \phi_h^{F_3} \circ \phi_{h/2}^{F_2} \circ \phi_{h/2}^{F_1}$ in Eq. (6) applied to the test system (13), M is expressed as

$$M_s(h) = M_s^1(h/2) M_s^2(h/2) M_s^3(h) M_s^2(h/2) M_s^1(h/2), \quad (15)$$

where $M_s^1(h/2) = \begin{bmatrix} I & h/2I \\ \mathbf{0} & I \end{bmatrix}$, $M_s^2(h/2) = \begin{bmatrix} I & \mathbf{0} \\ -\epsilon h^2 \lambda^2 / (2\gamma_0) I & I \end{bmatrix}$, and $M_s^3(h) = \begin{bmatrix} I & \mathbf{0} \\ \mathbf{0} & O(h\omega/\gamma_0) \end{bmatrix}$

are four-dimensional matrices, and $O(h\omega)$ is a rotation matrix $O(a) = \begin{bmatrix} \cos(a) & \sin(a) \\ -\sin(a) & \cos(a) \end{bmatrix}$.

If replacing $h\omega$ with $2 \arctan(h\omega/2)$ in Eq.(15), we can get the evolution matrix of the method \tilde{G}_h^2 in Eq. (7).

It is presented that a volume-preserving method applied to a source free system is linearly stable if and only if the eigenvalues of the update matrix have modulus 1 [8]. In Fig. 1, we display the stability domain of the second order volume-preserving methods with respect to $\epsilon h \lambda / \sqrt{\gamma_0}$ and $h\omega / (\gamma_0 \pi)$, where the left bottom region of the blue dashed line indicates the physical unstable region of the test system.

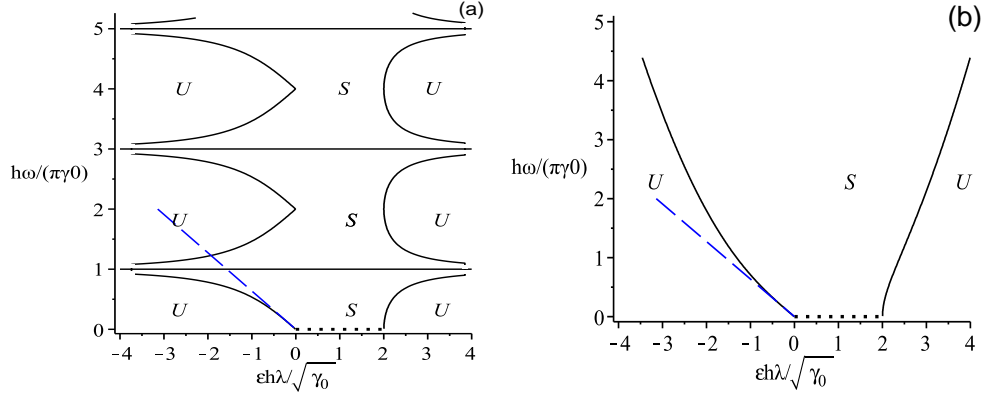


FIG. 1. Stability domain of second order volume-preserving numerical methods. Left(a): The method G_h^2 in Eq.(6); Right(b): The method \tilde{G}_h^2 in Eq.(7). The abscissa represents $\epsilon h \lambda / \sqrt{\gamma_0}$, and the ordinate represents $h\omega / (\gamma_0 \pi)$. Here λ^2 reflects the dimensionless value $\mathbf{E}(\mathbf{x}_0) / B_0 c$, ω reflects the dimensionless value $B(\mathbf{x}_0) / B_0$, and $\gamma_0 = (\sqrt{1 + p_0^2})^3$. The solid curves are boundaries of the stability domain. ‘S’ labels stable region, ‘U’ labels unstable region. The left bottom region below the dashed line $\omega = -2\epsilon \lambda \sqrt{\gamma_0}$ is the unstable region of the test system.

From the observation of Fig. 1, we get the following results:

1. When $\epsilon = 1$, both of the two schemes are stable if $h \lambda / \sqrt{\gamma_0} < 2$, i.e., $h < 2\sqrt{\gamma_0} / \lambda$. This means that if γ_0 is large or λ is small, the larger h can be taken to guarantee that the second order SVP methods are still linearly stable. It is noticed that larger $\gamma_0 = (\sqrt{1 + p_0^2})^3$ implies larger kinetic energy.

2. If the two schemes \tilde{G}_h^2 and G_h^2 are applied to a problem with uniform electric field, i.e., $\lambda = 0$, they are unconditionally stable. Moreover, for the case when the electric field changes slowly in space, i.e. λ is small enough the schemes \tilde{G}_h^2 and G_h^2 can be stable for a very large h . In the practical computation due to the Nyquist limit we need the time step h satisfying $h\omega/(\gamma_0\pi) \leq 1$ in order to simulate accurately the Larmor cyclotron.
3. From the two plots in Fig.1, it is observed that the stability domain of the method G_h^2 is 2π periodic with respect to $h\omega/\gamma_0$, while for the method \tilde{G}_h^2 the domain becomes larger along with the increasing $h\omega/\gamma_0$ in $[0, 5\pi]$. It is known that the slope of the line across the origin of coordinate is $s = \omega/(\sqrt{\gamma_0}\pi\lambda)$. With λ , ω and γ_0 satisfying $s < 0.52$, the stability domain shown in Fig. 1 implies that the method G_h^2 allows a larger time step than one for the method \tilde{G}_h^2 .

In Fig. 2, the stability of the fourth order method G_h^4P in Eq. (11) are compared with the composed methods G_h^4Y in Eq. (8) and G_h^4S in Eq. (9). It is observed that compared with the second order method G_h^2 in Fig. 1(a), the fourth order Suzuki composition G_h^4S has an enlarged stability domain in Fig. 1(b), while the Yoshida composition has a shrunk stability domain in Fig. 1(a). Among the three methods, the processed method G_h^4P has the largest stability domain shown in (c). This verifies that the processed method allows both higher order of accuracy and larger threshold of the time step h .

IV. NUMERICAL EXPERIMENTS

In this section, the SVP methods presented in the above section are applied to simulate the relativistic problems with different electromagnetic fields.

Example 1. Consider the relativistic dynamics of a charged particle in the Penning trap. For this problem, the electromagnetic field is given by

$$\mathbf{B} = B_0\mathbf{e}_z, \quad \mathbf{E} = -\epsilon E_l \left(\frac{x}{R_0}\mathbf{e}_x + \frac{y}{R_0}\mathbf{e}_y \right),$$

where $B_0 = 1T$, $E_l = 3V/m$, and $R_0 = 1m$.

We first simulate the relativistic dynamics of an electron in the ideal penning trap with $\epsilon = 1$. We take the initial momentum as $\mathbf{p}_{0\parallel} = 0.1m_0c$, $\mathbf{p}_{0\perp} = 0.5m_0c$, and the initial

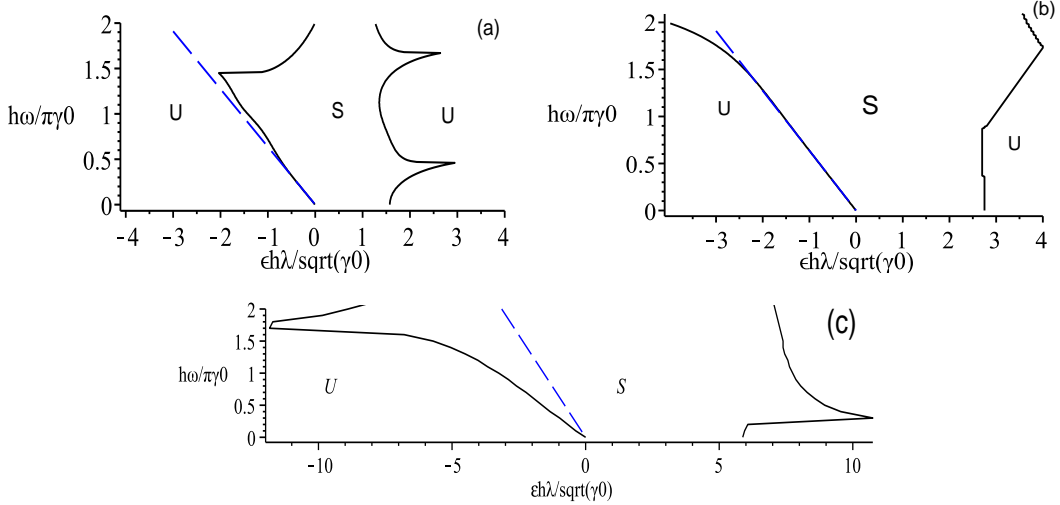


FIG. 2. Stability domain of the fourth order volume-preserving methods. (a) The Yoshida composition based on the method G_h^2 ; (b). The Suzuki composition method based on G_h^2 . (c). The processed fourth order method $G_h^4 P$. Here, λ , ω and γ_0 are defined as above.

position as $\mathbf{x} = 0.3l_0\mathbf{e}_x - l_0\mathbf{e}_y$. After normalizing the temporal variables by $T_0 = m_0/(eB_0) = 5.7 \times 10^{-12}s$, and the spatial variables by $l_0 = m_0c/(eB_0)$, the dimensionless field parameters is (N denotes the normalized variable)

$$\mathbf{B}_N = \omega\mathbf{e}_z, \mathbf{E}_N = -\lambda^2 \left(\frac{x}{R_0}\mathbf{e}_x + \frac{y}{R_0}\mathbf{e}_y \right), \text{ with } \omega = 1, \lambda = 10^{-4}.$$

In this experiment, as the initial kinetic energy is bounded and close to 1, we choose $\gamma_0 = 1$ in the test equation Eq. (13). As $\epsilon = 1$, and the slope $s = \omega/(\lambda\sqrt{\gamma_0}\pi) = 10^4/\pi$ is large enough, from Fig. 1 we can see that the two second order SVP methods G_h^2 and \tilde{G}_h^2 are stable regardless of h . Thus the step size should be chosen in $h \leq \gamma_0\pi/\omega = \pi$ according to the Nyquist limit.

In Fig. 3, we show the numerical results computed by the SVP methods running over 8000 steps with $h = 0.3\pi = 5.37 \times 10^{-12}s$. The explicit fourth order method RK4 is calculated as a comparison. It is known that the exact orbit of the particle is an nearly closed orbit with radius $p_\perp/(m_0c) \approx 0.5$. It is observed from Fig. 3(a) that the SVP method can simulate the orbit well. The relative energy error displayed in Fig. 3(b) is bounded up to 10^{-14} during the entire simulation time. Conversely, Fig. 3(b) and (c) show that the numerical orbit spirals inside and the energy error is damping. This is because of that the numerical solution computed by RK4 scheme has the non-stability in long term computations.

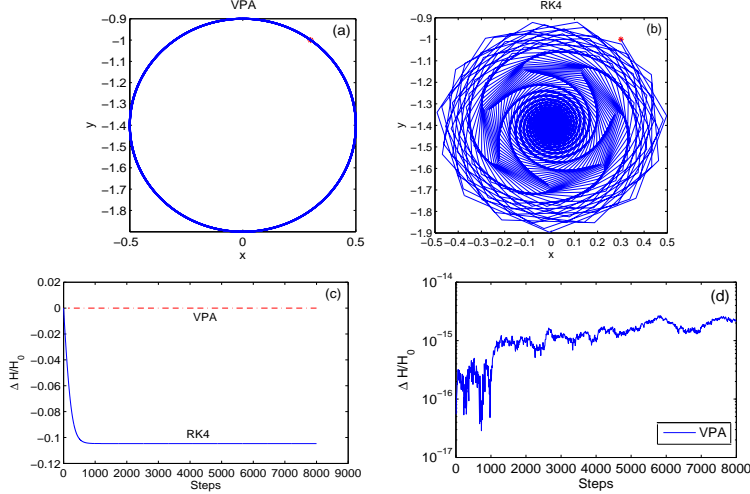


FIG. 3. The simulation result of the relativistic dynamics of a particle in an ideal penning trap. The SVP methods and RK4 are iterated for 8000 steps with the step size $h = 0.3\pi$. (a): Orbit by the SVP methods. (b): Orbit by RK4. (c) and (d): Energy error as a function of steps.

In Fig. 4, the global errors of the dimensionless position variables computed by the second and fourth order methods are compared. Fig. 4(a) and Fig. 4(c) display the errors as a function of time step h , which verifies the orders of the SVP methods. In Fig. 4(a), the method G_h^2 is more accurate than the method \tilde{G}_h^2 because of the smaller error constant. In Fig. 4(c), it is clear that the processed fourth order method is the most accurate. Fig. 4 (b) and Fig. 4(d) display the errors as a function of the computing efforts, which are counted by the number of the evaluations of \mathbf{E} . It is observed that if the given tolerance on numerical errors is less than 0.01%, the fourth order methods need less computing efforts than the second order methods. Among the fourth order methods, the processed method $G_h^4 P$ is the cheapest.

Next we study the long-term performances of the SVP methods in the case with time-dependent electromagnetic fields. The problem possessing a plane polarized electromagnetic wave (see Ref. 33) is considered. After normalizing the variables as before, we choose the dimensionless fields to be

$$\mathbf{E} = E_y \mathbf{e}_y, \mathbf{B} = B_z \mathbf{e}_z, E_y = B_z = 3 \sin(3(t - x)).$$

In this case, the evolution of the particle energy $W(\mathbf{p})$ satisfies

$$I(t) = W(\mathbf{p}(t)) - p_x(t) = \text{constant},$$

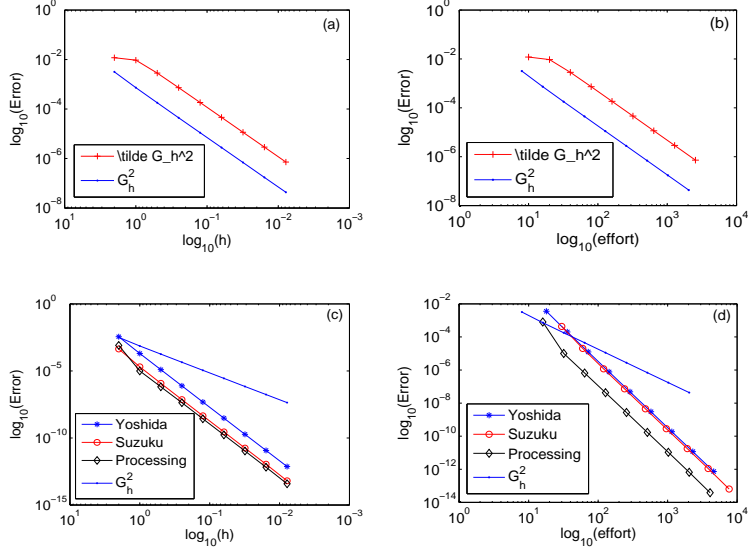


FIG. 4. Relative errors of the dimensionless position variables in the experiment with an ideal penning trap. (a) and (c): Errors as a function of the time step h ; (b) and (d): Errors as a function of the the computing amount (counted by evaluations of \mathbf{E}). (a) and (b): Errors of the 2nd order methods; (c) and (d): Errors of the 4-th order methods compared with second order method G_h^2 .

where p_x represents the momentum in the x -direction. Set the initial position and momentum to be $\mathbf{x}_0 = 0.3\mathbf{e}_x + 0.2\mathbf{e}_y$, $\mathbf{p}_0 = 0.4\mathbf{e}_x + 0.3\mathbf{e}_y + 0.1\mathbf{e}_z$, we run the second order SVP methods for 10^6 steps with the step size $h = 0.1$. The fourth order Runge-Kutta method is used as a comparison. The results are shown in Fig. 5. From Fig. 5(a) we can see that the relative error of RK4 is smaller than that of the SVP method at the beginning few steps, but it grows over 1% rapidly. Meanwhile the relative error of SVP methods stays below 0.5% over the entire simulation time. In Fig. 5(b) the invariant $I(t)$ is preserved approximately by the SVP method, while the invariant computed by RK4 is dissipated. It can be verified that for the long-term simulation the two second order SVP methods are linearly and nonlinearly stable.

V. CONCLUSION

We have constructed high order volume-preserving methods for the relativistic dynamics of a charged particle by the splitting technique with processing. For the system with time-

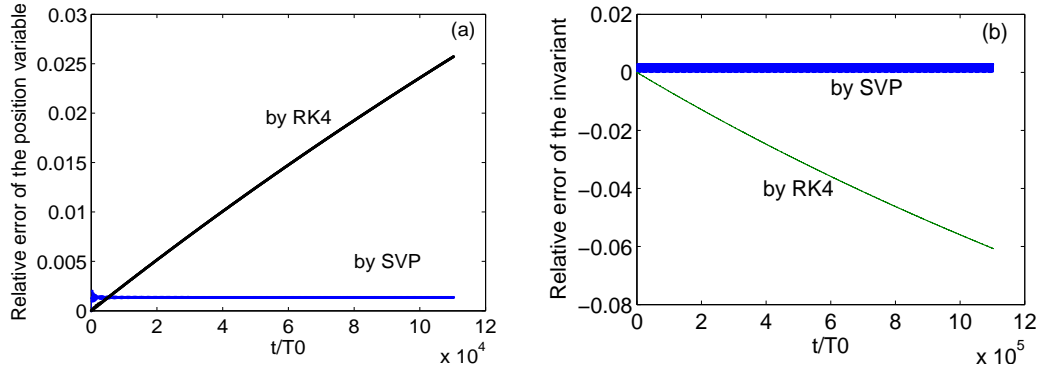


FIG. 5. The long-term simulation result of the relativistic dynamics of a particle under a plane polarized electromagnetic wave. The step size is $h = 0.1$. (a): Relative error of the position variables $\|\mathbf{x}_n - \mathbf{x}(nh)\|/\|\mathbf{x}(nh)\|$ as a function of normalized time t/T_0 ; (b): Relative error of the invariant $I(t)$.

dependent fields, we reformulate the system by extending its dependent variables space to include time t . With the newly derived system, we give a valid construction procedure of the symmetric volume-preserving methods. We have employed the processing technique to present the efficient methods with high order of accuracy. Linear stability which can serve as a hint on the choice of time step size of the SVP methods are analyzed. Numerical experiments show that the SVP methods are accurate and conservative for the long term tracking of the trajectory of relativistic particles.

ACKNOWLEDGMENTS

This research was supported by ITER-China Program (2015GB111003, 2014GB124005), JSPS-NRF-NSFC A3 Foresight Program in the field of Plasma Physics (NSFC-11261140328), the National Science Foundation of China (11271357, 11575186, 11575185, 11505185, and 11505186), the Foundation for Innovative Research Groups of the NNSFC (11321061), the Fundamental Research Funds for the Central Universities (WK2030040057).

-
- [1] H. Qin and X. Guan, Physical Review Letters **100**, 035006 (2008).
 - [2] H. Qin, X. Guan, and W. M. Tang, Physics of Plasmas **16**, 042510 (2009).

- [3] H. Qin, S. Zhang, J. Xiao, J. Liu, Y. Sun, and W. M. Tang, *Physics of Plasmas* **20**, 084503 (2013).
- [4] J. Squire, H. Qin, and W. M. Tang, *Physics of Plasmas* **19**, 084501 (2012).
- [5] S. A. Chin, *Phy. Rev. E* **77**, 066401 (2008).
- [6] J. M. Finn and L. Chacón, *Physics of Plasmas* **12**, 054503 (2005).
- [7] Y. He, Y. Sun, J. Liu, and H. Qin, *Journal of Computational Physics* **281**, 135 (2015).
- [8] Y. He, Y. Sun, J. Liu, and H. Qin, *Journal of Computational Physics* **305**, 172 (2016).
- [9] R. Zhang, J. Liu, H. Qin, Y. Wang, Y. He, and Y. Sun, *Physics of Plasmas*, Submitted (2015).
- [10] J. Xiao, J. Liu, H. Qin, and Z. Yu, *Physics of Plasmas* **20**, 102517 (2013).
- [11] M. Kraus, *Variational Integrators in Plasma Physics*, Ph.D. thesis, Technical University of Munich (2014).
- [12] Y. Zhou, H. Qin, J. W. Burby, and A. Bhattacharjee, *Physics of Plasmas* **21**, 102109 (2014).
- [13] B. A. Shadwick, A. B. Stamm, and E. G. Evstatiev, *Physics of Plasmas* **21**, 055708 (2014).
- [14] E. Evstatiev and B. Shadwick, *J. Comput. Phys.* **245**, 376 (2013).
- [15] H. Qin, J. Liu, J. Xiao, R. Zhang, Y. He, Y. Wang, Y. Sun, J. W. Burby, L. Ellison, and Y. Zhou, *Nuclear Fusion* **56**, 014001 (2016).
- [16] J. Xiao, H. Qin, J. Liu, Y. He, R. Zhang, and Y. Sun, *Physics of Plasmas* **22**, 112504 (2015).
- [17] Y. He, Y. Sun, Z. Zhou, J. Liu, and H. Qin, arXiv:1509.07794 (2015).
- [18] R. D. Ruth, *IEEE Trans. Nucl. Sci* **30**, 2669 (1983).
- [19] K. Feng, in *the Proceedings of 1984 Beijing Symposium on Differential Geometry and Differential Equations*, edited by K. Feng (Science Press, 1985) pp. 42–58.
- [20] K. Feng and M. Qin, *Symplectic Geometric Algorithms for Hamiltonian Systems* (Springer-Verlag, 2010).
- [21] E. Hairer, C. Lubich, and G. Wanner, *Geometric Numerical Integration: Structure-Preserving Algorithms for Ordinary Differential Equations* (Springer, New York, 2003).
- [22] Z. Shang, *Numer. Math.* **83**, 477496 (1999).
- [23] C. Ellison, J. Burby, and H. Qin, *Journal of Computational Physics* **301**, 489 (2015).
- [24] J. Qiang, M. Furman, and R. Ryne, *Journal of Computational Physics* **198**, 278 (2004).
- [25] K. Feng and Z. Shang, *Numer. Math.* **71**, 451 (1995).
- [26] S. Blanes, F. Casas, and J. Ros, *SIAM J. Sci. Comp.* **21**, 711 (1999).

- [27] S. Blanes, F. Casas, and A. Murua, *SIAM J. Sci. Comp.* **27**, 1817 (2006).
- [28] S. Blanes, F. Diele, C. Marangi, and S. Ragni, *Journal of Computational and Applied Mathematics* **235**, 646 (2010).
- [29] K. Feng and Z. Shang, *Numer. Math.* **71**, 451 (1995).
- [30] R. I. McLachlan and G. R. W. Quispel, *Acta Numer.* **11**, 341 (2002).
- [31] H. Yoshida, *Phys. Lett. A.* **150**, 262 (1990).
- [32] M. Suzuki, *Phys. Lett. A* **165**, 387 (1992).
- [33] E. M. McMillan, *Phys. Rev.* **79**, 498 (1950).